Chemical Physics Letters 536 (2012) 9–13

Contents lists available at SciVerse ScienceDirect

Chemical Physics Letters

journal homepage: www.elsevier.com/locate/cplett

Methane bond activation by Pt and Pd subnanometer clusters supported on graphene and carbon nanotubes

John Russell [a,c], Peter Zapol [c,*], Petr Král [a,b], Larry A. Curtiss [c]

[a] Department of Chemistry, University of Illinois at Chicago, Chicago, IL 60607, United States
[b] Department of Physics, University of Illinois at Chicago, Chicago, IL 60607, United States
[c] Materials Science Division, Argonne National Laboratory, Argonne, IL 60439, United States

ARTICLE INFO

Article history:
Received 3 January 2012
In final form 22 March 2012
Available online 31 March 2012

ABSTRACT

Activation of the C–H bond is important for hydrocarbon catalysis with applications in energy technology such as production of synthetic fuels. Subnanometer clusters such as Pt_4 show great promise for catalytic activities potentially much greater than monolith. Using density functional theory, we investigated C–H bond breaking, an important step of the conversion reaction of methane to liquid fuels, on Pt and Pd subnanometer clusters with graphene and carbon nanotubes as supports. Our results show that CNT supports can be selected by size and chirality to provide stable support for subnanometer Pt and Pd clusters and tailor their catalytic activity.

1. Introduction

The activation of alkanes is an important challenge due to limited fossil fuel reserves and increasing global demand for petrochemicals [1]. Renewable energy sources in the future may still require that energy be stored as liquid fuels for transportation. Highly selective, efficient and robust catalysts are therefore important to meet this challenge, and are an active area of research. C–H bond activation in CH_4 provides a good model chemistry for similar bond activation in other alkanes.

Subnanometer Pt clusters on Al_2O_3 show great promise with catalytic activities much greater than Pt monolith [2] due to undercoordination of Pt atoms and high surface area to volume ratio in the clusters. Carbon nanotubes (CNTs) and graphene have also been proposed as supports for transition metal catalysts [3–6], including palladium [7] and platinum tetramers [8], due to their high surface area and capability to stabilize these clusters [9]. Recent experimental advances in the separation of single chirality CNTs [10,11] raise the possibility of matching catalytic materials such as subnanometer clusters to select CNT supports to improve catalytic potential of the combined system. A key question is whether the adsorption on a support will modify the catalytic activity of subnanometer clusters due to the formation of cluster–support bonds which increases coordination of the cluster atoms. We investigate the role of CNT curvature and chirality for methane C–H bond activation on CNT-supported Pt and Pd tetramers using first principles methods.

2. Methods

Methane activation by supported Pt and Pd tetramers was investigated with a first-principles approach using density functional theory (DFT) with the B3LYP hybrid functional [12,13] as implemented in the Gaussian09 software package [14]. A generalized (5*d*, 7*f*) 6-31G* basis set was used for carbon and hydrogen atoms in the methane and support structure, while Stuttgart 'SDD' effective core potentials and corresponding basis sets were used for Pt and Pd atoms of the clusters. The support was represented by a 66-carbon atom graphene model with edges terminated by 22 hydrogen atoms, either flat or bent to CNT curvature, the latter being shown in Figure 1 for a (7,0) CNT. We investigated nine support structures including graphene, (10-10), (15-0), (8-8), (10-0), (5-5), (8-0), (7-0) and (4-4) CNTs in order of increasing curvature.

The support structure for a given curvature r^{-1} was produced by a linear transformation which mapped the planar graphene to a cylinder of radius r such that $x_2 = r\cos\left(\frac{x}{r}\right)$, $y_2 = y_1$, and $z_2 = r\sin\left(\frac{x}{r}\right)$. The radius r is given as,

$$r_0 = \sigma\frac{\sqrt{3(n^2+nm+m^2)}}{2\pi}, \quad (1)$$

where n and m are the lattice vectors and σ is the carbon–carbon covalent bond length (σ = 1.41 Å) [15]. We studied CNTs of both zigzag (n,0) and armchair (n,n) chiralities, where the graphene is rotated by 90° before bending. The geometry was then optimized with the hydrogen atoms fixed to hold the curvature, and the carbon atoms were allowed to relax. The optimized structures were calculated with unrestricted spin, however the lowest energy spin configurations were closed shell singlet in all cases. The energy

* Corresponding author.
E-mail address: zapol@anl.gov (P. Zapol).

0009-2614/$ - see front matter © 2012 Elsevier B.V. All rights reserved.
http://dx.doi.org/10.1016/j.cplett.2012.03.080

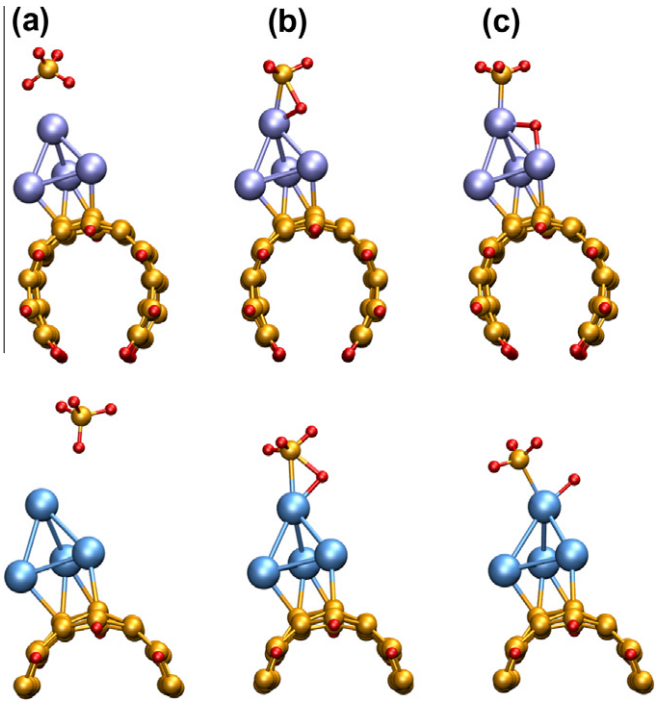

Figure 1. Calculated structures of a methane molecule reacting with a palladium tetramer (top row), supported on a (7,0) CNT represented by a finite model: (a) molecular adsorption, (b) transition state, (c) dissociative adsorption. A methane molecule reacting with a platinum tetramer using the same model (bottom row, truncated) shows hydrogen adsorption on a single Pt atom rather than occupying a bridge site as for the Pd tetramer.

required to bend the support to the shape of the CNT has quadratic dependence on r, as expected. The relative energy of bending where $\Delta E = E_b - E_{\text{flat}}(\text{eV})$ can be fit such that $\Delta E = 127.666\, r^{-2}(\text{Å}^{-2})$ with RMS deviation of 0.068 eV.

The optimized support structure was then combined with the metal clusters to find the binding energies of the cluster to the support. All cluster–support structures were optimized in both singlet and in triplet states. Cluster stability on the CNT support was evaluated by calculating the binding energy, E_B:

$$E_B^{\text{M}} = E_{(\text{M}_4-\text{CNT})} - E_{\text{M}_4} - E_{\text{CNT}}, \tag{2}$$

where metal M is Pd or Pt, $E_{(\text{M}_4-\text{CNT})}$ is the total energy of the combined cluster–support system, E_{M_4} is the energy of the (triplet) cluster, and E_{CNT} is the energy of the (singlet) support. Negative E_B energies are exothermic.

Next, methane was added to the lowest-energy singlet and triplet configurations of the cluster–support systems and then optimized to find both molecular adsorption (MA) and dissociative adsorption (DA) of the methane on the supported cluster. The energy of adsorption, $E_{\text{MA(DA)}}$, was calculated by,

$$E_{\text{MA(DA)}}^{M} = E_{(\text{CH}_4-\text{M}_4-\text{CNT})}^{\text{MA(DA)}} - E_{(\text{M}_4-\text{CNT})} - E_{\text{CH}_4}, \tag{3}$$

where $E_{(\text{CH}_4-\text{M}_4-\text{CNT})}^{\text{MA(DA)}}$ is the total energy of the combined methane–cluster–support system in the configuration corresponding to either MA or DA, and E_{CH_4} is the total energy of the methane. Negative $E_{\text{MA(DA)}}$ energies are exothermic.

Finally, the transition state (TS) was found by optimization using the Berny Algorithm [16]. The apparent barrier, E_a^{M} is given as,

$$E_a^{\text{M}} = E_{\text{TS}}^{\text{M}} - E_{(\text{M}_4-\text{CNT})} - E_{\text{CH}_4}, \tag{4}$$

where E_{TS}^{M} is the total energy in the transition state. Negative E_a^{M} energies are possible provided that $E_{\text{TS}}^{\text{M}} > E_{\text{MA}}^{\text{M}}$, which indicates no apparent barrier.

3. Results

3.1. Cluster–nanotube binding

The cluster binding energies to the support, E_B, are shown in Figure 2. The trend is that E_B increases with CNT curvature for both Pd and Pt. Additionally, optimized geometries show a trend in which the number of cluster–support bonds increases with curvature. This is not surprising due to the greater reactivity of small CNTs which are highly strained [17,18]. Our results show that for triplet Pd_4–CNT systems, clusters bind more strongly to zigzag CNT supports than to armchair CNT supports with the exception of the (10,0) CNT. The opposite result is obtained with singlet Pd_4–CNT systems. In contrast, in triplet Pt_4–CNT systems, clusters bind more strongly to armchair CNT supports than to zigzag supports except at very high curvature of $r^{-1} > 0.3$ Å^{-1}. But in singlet Pt_4–CNT systems, clusters bind more strongly to zigzag CNT supports than to armchair CNT supports. This shows that electronic effects of the support play a role in the binding properties of the cluster as armchair CNTs are metallic and zigzag CNTs are mostly semiconducting [19].

Our results using the B3LYP hybrid functional show that Pd_4 and Pt_4 cluster–CNT systems have stronger binding energies in the triplet state than in the singlet state. These results are in agreement with previous DFT studies with the GGA-PBE functional [8] that showed Pt_4 stability on (10,0) CNTs with binding of 2.31 eV and on graphene with binding of 1.35 eV, both in singlet states. The lowest energy Pt_4 binding configuration calculated with the GGA-PBE functional has three surface bonds to either (10,0) CNT or graphene supports, which is similar to that found with the B3LYP hybrid functional.

3.2. Methane activation by unsupported clusters

We use the gas phase Pd_4 and Pt_4 clusters as a reference for comparison with the clusters supported on CNTs shown in Figure 1. The comparison is appropriate to determine the effect of the support on catalytic activity because the additional bonds from the cluster to the support may reduce the undercoordination that is characteristic of subnanometer cluster activity.

The lowest energy configurations of unsupported Pd_4 and Pt_4 gas phase clusters are trigonal pyramids in triplet states. In Figure 3, we show the spin density of Pd_4 reacting with methane. The reaction starts with methane and the cluster separated, and proceeds from MA, to the C–H bond insertion TS, and finally to DA. The unpaired spin density resides on the cluster throughout the reaction with very little contribution from the carbon atom.

The C–H bond breaking reaction is endothermic on Pd_4 clusters but is exothermic on a Pt_4 cluster as shown in Figure 3. The apparent barrier for breaking the C–H bond in methane adsorbed on a Pd_4 is 1.0 eV, and the dissociation is endothermic, by 0.9 eV. Conversely, the apparent barrier to C–H bond insertion on Pt_4 is much lower at 0.1 eV, and the dissociation is exothermic, by −0.56 eV. In comparison, other studies have found barriers for C–H bond breaking in methane to be 0.66 eV on a Pd (1 1 1) surface [20] and 0.74 eV on a Pt (1 1 1) surface [21,2]. Overall, this shows that Pt_4 has a higher activity than Pd_4 for C–H bond breaking of methane.

3.3. Reaction energies, islands of stability and instability

The size and chirality of the support can strongly effect the adsorption and dissociation of methane on subnanometer clusters.

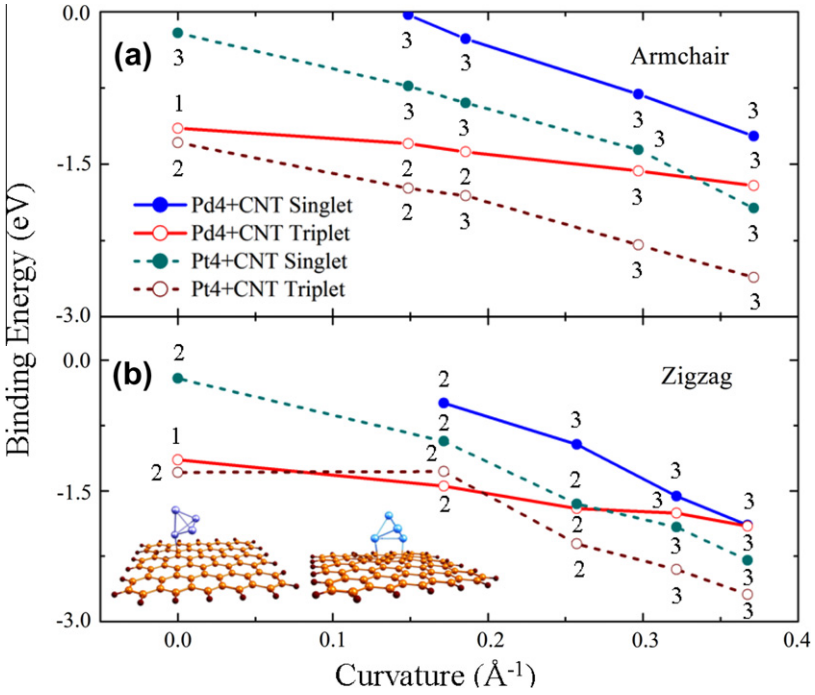

Figure 2. Calculated Pd_4/Pt_4 cluster binding energy E_B^M to the CNT support as a function of CNT curvature and chirality: (a) armchair and (b) zigzag. The number of surface bonds from the cluster to the support are shown next to each point. Inset: a Pd_4 cluster with one surface bond to graphene (left) and a Pt_4 cluster with two surface bonds to graphene (right).

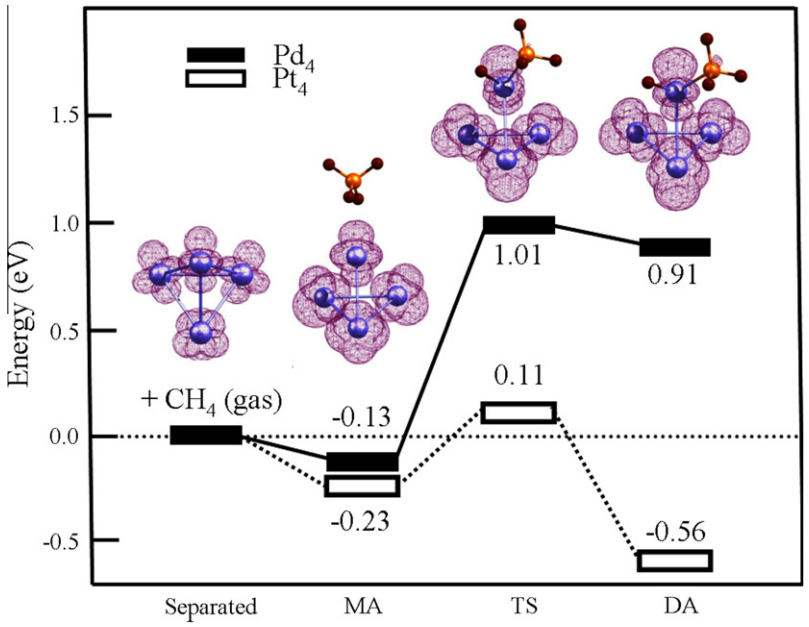

Figure 3. Adsorption energies and reaction barriers of C–H bond breaking which proceeds from the separated methane and unsupported Pd (Pt) tetramers, to molecular adsorption (MA) of the methane, to the transition state (TS) of C–H bond insertion, and finally to dissociative adsorption (DA). Inset spin density plots of the Pd tetramer shows very little contribution of spin density from the methane throughout the reaction. All energies are relative to $M_4 + CH_4$ and spin density ($\alpha - \beta$) isosurface contour values are 0.003 e^-/α_0^3.

The energies of adsorption, E_{MA}^M and E_{DA}^M, are shown as a function of curvature in Figure 4, for methane adsorbed on Pd_4 and Pt_4 clusters supported by armchair and zigzag CNTs and graphene. In all cases the reaction on Pd is endothermic because $E_{DA}^{Pd} > E_{MA}^{Pd}$. However, the trend of the reaction energy is less endothermic for small diameter CNTs for both zigzag and armchair chiralities as the difference between E_{DA}^{Pd} and E_{MA}^{Pd} decreases with curvature, though not monotonically. In contrast, the reaction on Pt is exothermic for graphene and CNTs of large diameter where $E_{DA}^{Pt} < E_{MA}^{Pt}$.

The trends in adsorption energies, E_{MA}^M and E_{DA}^M, for Pd and Pt clusters are related to the cluster binding energy to the support, E_B^M. Cluster binding energy E_B^{Pd} ranges from −1.1 to −1.9 and E_B^{Pt} ranges from −1.3 to −2.7 eV for graphene to (7,0) CNT supports as shown in Figure 2. The least endothermic Pd_4 reaction occur

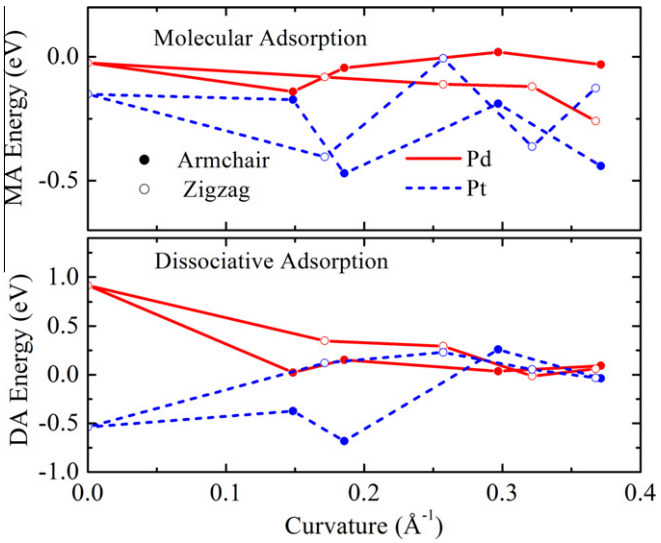

Figure 4. Energies of molecular adsorption (MA), E^{M}_{MA}, and dissociative adsorption (DA), E^{M}_{DA}, for tetramer clusters where M is Pd (straight) or Pt (dashed), as a function of support curvature and chirality, including graphene ($r^{-1} = 0.0$ Å), zigzag (open circles) and armchair (filled circles) CNTs. The C–H bond insertion reaction is exothermic if $E^{M}_{DA} < E^{M}_{MA}$.

when the Pd cluster is strongly bound (−1.5 to −1.75 eV) to a small diameter CNT support. Conversely, the most exothermic Pt_4 reaction occurs when the Pt cluster is weakly bound (−1.7 and −1.8 eV) to a large diameter CNT support.

Moreover, the reaction is more exothermic on CNTs of particular sizes and chiralities, which might be understood as islands of stability. For Pd, the least endothermic reaction is for sizes that are tightly curved (5,5) armchair and (7,0) zigzag CNTs. Likewise for Pt, the most favorable sizes are (10,10) and (8,8) armchair CNTs. The least favorable size and chirality, an island of instability, for methane C–H bond insertion reactions on Pt are (15,0) CNTs.

We postulate that the reason some supports have lower or higher adsorption energies is due to geometric distortion and electronic effects of the support. The bond energy of the metal–CNT bond increases with curvature. However, the increased metal–CNT bond energy is off-set by distortion of the CNT and the cluster away from an optimal geometry in order to fit multiple binding sites on the support. We define the distortion energy as the difference in energy between the support (cluster) optimized in the reaction steps and the initial relaxed configuration. For both Pd_4 and Pt_4 clusters, the distortion energy for the support is inversely proportional to the support radius. Distortion energies ranged from 0.049 to 0.497 eV for triplet Pd_4 barriers and from 0.242 to 0.877 eV for triplet Pt_4 barriers, with graphene having the least distortion and (7,0) CNTs having the greatest distortion. A qualitative description of the calculated distortion energies is that cluster and CNT distortion is greater for adsorption on zigzag CNTs than on armchair CNTs.

3.4. Methane activation by clusters on concave support

We explore the reactivity and stability of catalysts on the inside of CNTs because of interest in using CNTs as nanoreactors, although our model is limited to large diameter CNTs. First, we compare Pt cluster binding to the concave side of a (10,10) model support with our results for the convex surface. A singlet Pt_4 binds with −0.5 eV to the concave support, compared to −0.7 eV to the convex side. A triplet Pt_4 binding is much weaker to the concave side with a binding energy of −0.9 eV, compared to a binding energy of −1.7 eV on the convex side.

Reaction energies on the concave (10,10) model CNT support are similar to those found on the convex side. Molecular and dissociative adsorption energies and the adsorption energies for triplet Pt_4 are −0.14 and −0.40 eV, respectively. Therefore, the reaction energies for C–H bond breaking on a triplet concave-(10,10) CNT supported Pt_4 cluster is −0.27 eV, slightly more exothermic than the reaction on the outer side of the CNT wall.

Overall this shows that the Pt clusters would likely be more stable on the outer CNT surface and less stable on the inside of a CNT support. The reaction energies for methane dissociation are comparable for clusters on the inner and outer surfaces of the CNT. A possible explanation for the weaker cluster binding to the concave CNT wall is that steric strain of the CNT creates greater electron density on the CNT exterior surface compared to the interior surface as the carbon atoms gain more sp^3 character with increasing CNT curvature.

3.5. C–H bond activation in methane

The apparent barriers, E^{M}_{a}, for methane C–H bond insertion on supported Pd_4 and Pt_4 clusters are shown as a function of support curvature and chirality in Figure 5. The trends in the apparent barriers, E^{M}_{a}, can be compared to those of the cluster–support binding energies, E^{M}_{B}, as shown in Figure 2. For Pd, the apparent barrier E^{Pd}_{a} has, approximately, a direct relationship to the binding energy E^{Pd}_{B}. A strongly bound (−1.9 eV) Pd_4 on a high curvature (4,4) CNT has an apparent barrier of 0.5 eV, which is half the apparent barrier of an unsupported Pd_4 cluster as shown in Figure 3. The trend in Pd apparent barrier, E^{Pd}_{a}, with chirality is less clear. Armchair CNTs have lower barriers at curvature below 0.18 Å^{-1} and zigzag CNTs have lower apparent barriers otherwise.

In contrast, the trend in the Pt apparent barriers, E^{Pt}_{a} with curvature is roughly opposite with barrier energies E^{Pt}_{a} decreasing with binding energies E^{Pt}_{B}. However, the trend is not linear and the Pt_4 cluster on a large curvature (8,8) CNT with relatively weaker binding (−1.8 eV) has the lowest apparent barrier of −0.1 eV, which is better than the unsupported Pt_4 cluster with an apparent barrier of 0.1 eV. Apparent barriers for Pt C–H bond activation E^{Pt}_{a}, are lower for armchair CNTs than for zigzag CNTs except at very high curvature above 0.3 Å^{-1}. The trends for reaction barriers with chirality are similar to the trends in adsorption energies, E^{Pt}_{MA} and E^{Pt}_{DA} with chirality.

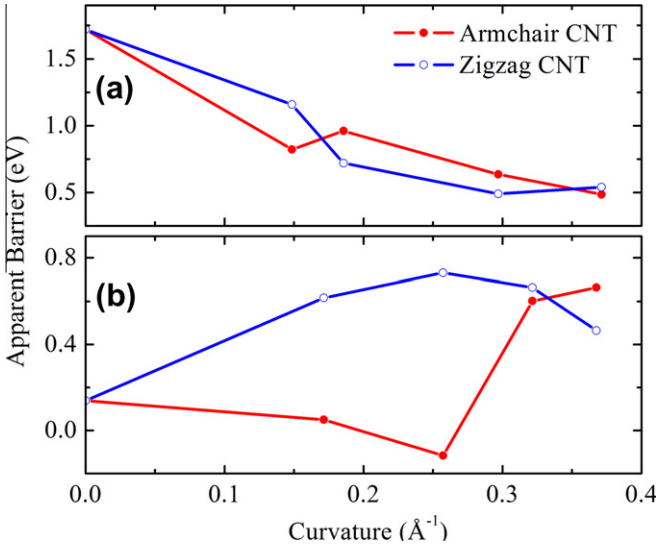

Figure 5. Calculated apparent barriers, E^{M}_{a}, for CH bonds with (a) M = Pd_4 and (b) M = Pt_4 catalysts on supports by curvature and chirality, including graphene ($r^{-1} = 0.0$ Å), armchair, and zigzag CNTs. Barriers are reduced for Pd clusters by CNT supports and increased for Pt clusters relative to gas phase (shown in Figure 3).

4. Conclusions

Both Pt and Pd subnanometer clusters are stable on CNT supports with binding energies for Pt higher than for Pd. In the triplet state, Pt and Pd have opposite ordering of binding energies relative to the chirality of the support, with armchair supports having lowest energy for Pt_4 and with zigzag supports having lowest energy for Pd_4. This pattern is reversed in the higher energy singlet state. Reaction energies for CH_4 dissociation on supported Pd clusters are more exothermic relative to gas phase Pd_4 while reaction energies on supported Pt clusters are less exothermic relative to gas phase Pt_4. When compared to an initial state of a bound cluster–support system with a separated methane, all reactions on supported Pd_4 are endothermic and all reactions on supported Pt_4 are exothermic except for highly curved armchair supports. In all cases, triplet states for products are preferred. For Pd clusters, barriers for C–H bond activation decrease with increasing CNT curvature, while the trend is opposite for Pt clusters. Certain CNT sizes and chiralities result in lower barriers than the overall trend. Our results show that CNT supports can be selected by size and chirality to provide stable support for subnanometer Pt and Pd clusters and tailor their catalytic activity.

Acknowledgments

The authors acknowledge the use of Argonne LCRC and the Center for Nanoscale Materials computer resources. Work was supported by the US Department of Energy, Office of Science, Office of Basic Energy Sciences, under Contract No. DE-AC02-06CH11357.

References

[1] J. Labinger, J. Bercaw, Nature 417 (2002) 507.
[2] S. Vajda et al., Nat. Mater. 8 (2009) 213.
[3] A. Titov, P. Zapol, P. Král, D.J. Liu, H. Iddir, K. Baishya, L. Curtiss, J. Phys. Chem. C 113 (2009) 21629.
[4] N. Cuong, A. Fujiwara, T. Mitani, D. Chi, Comput. Mater. Sci. 44 (2008) 163.
[5] S. Kim, Y. Jung, S-J. Park, Colloids Surf. A 313–314 (2008) 189.
[6] S.R. Stoyanov, A. Titov, P. Král, Coor. Chem. Rev. 253 (2009) 2852.
[7] T. Prasomsri, D. Shi, D.E. Resasco, Chem. Phys. Lett. 497 (2010) 103.
[8] N. Cuong, A. Sugiyama, A. Fujiwara, T. Mitani, D.H. Chi, Phys. Rev. B 79 (2009) 235417.
[9] T.W. Odom, J.H. Hafner, C.M. Lieber, Top. Appl. Phys. 80 (2001) 173.
[10] A.A. Green, M.C. Hersam, Adv. Mater. 23 (2011) 2185.
[11] M.C. Hersam, Nat. Nanotechnol. 3 (2008) 387.
[12] A.D. Becke, J. Chem. Phys. 98 (1993) 5648.
[13] C. Lee, W. Yang, R. Parr, Phys. Rev. B 37 (1988) 785.
[14] M.J. Frisch et al., Gaussian09, Revision A.1, Gaussian, Inc., Wallingford CT, 2009.
[15] B.J. Cox, J.M. Hill, Carbon 45 (2007) 1453.
[16] B. Schlegel, J. Comput. Chem. 3 (1982) 214.
[17] S. Park, D. Srivastava, K. Cho, Nano Lett. 3 (2003) 1273.
[18] D.A. Horner, P.C. Redfern, M. Sternberg, P. Zapol, L.A. Curtiss, Chem. Phys. Lett. 450 (2007) 71.
[19] X. Lu, Z. Chen, Chem. Rev. 105 (2005) 3643.
[20] Z.-P. Liu, P. Hu, J. Am. Chem. Soc. 125 (2003) 1958.
[21] A. Michaelides, P. Hu, J. Am. Chem. Soc. 122 (2000) 9866.